

# Electronic Supporting Information

## **A crystalline sponge based on dispersive forces suitable for X-ray structure determination of included molecular guests**

**Elena Sanna<sup>a</sup>, Eduardo C. Escudero-Adán<sup>b</sup>, Antonio Bauzá<sup>a</sup>, Pablo Ballester<sup>b</sup>,  
Antonio Frontera<sup>a</sup>, Carmen Rotger<sup>a</sup> and Antonio Costa<sup>a\*</sup>**

<sup>a</sup> Universitat de les Illes Balears, Palma, 07122, Spain.

<sup>b</sup> Institut of Chemical Research of Catalonia (ICIQ). Avda. Països Catalans 16, 43007  
Tarragona (Spain). Catalan Institute for Research and Advanced Studies (ICREA).  
Passeig Lluís Companys 23, 08010, Barcelona (Spain).

Email: [antoni.costa@uib.es](mailto:antoni.costa@uib.es); Fax: +34 971 172436; Tel: +34 971 173266.

## Table of contents

### 1. Experimental section

1a.	Instrumental methods	p 3
1b.	Materials and synthesis	p 4
1c.	$^{13}\text{C}$ CP-MAS spectra	p 8
1d.	TGA and DSC analysis	p 9
1e.	X-ray structure of <b>3(II)</b>	p 10
1f.	Crystal data of solvates and representative parameters	p 11
1g.	Quantitative determination of molar ratio <b>3</b> :guest by $^1\text{H}$ NMR	p 13

### 2. Theoretical section

2a.	Theoretical methods	p 15
-----	---------------------	------

## Supporting Information

### 1. Experimental Section

#### 1a. Instrumental Methods

**NMR.** Solution  $^1\text{H}$  and  $^{13}\text{C}$  spectra were recorded on Bruker AVANCE 300 ( $^1\text{H}$  at 300 MHz and  $^{13}\text{C}$  at 75 MHz) and on Bruker AVANCE III 600 ( $^1\text{H}$  at 600 MHz and  $^{13}\text{C}$  at 150.9 MHz) equipped with a cryoprobe, in  $\text{CDCl}_3$  using the residual proton signal as reference. Chemical shifts ( $\delta$ ) are in ppm and coupling constants ( $J$ ) in Hz.

**Thermogravimetric Analysis.** TG analyses were carried out using a SDT2960 TGA analyzer (TA instruments) with an automated vertical overhead thermobalance. The experiments were performed on 10 - 20 mg samples, over a temperature range of 25-600  $^\circ\text{C}$  at a constant heating rate of 10  $^\circ\text{C min}^{-1}$  with a purge of dry nitrogen flowing at 30  $\text{mL min}^{-1}$ . The samples were crushed, blotted dry and placed in open Pt pans for TG experiments.

**Differential Scanning Calorimetry.** DSC were carried out using a DSC2920 modulated DSC (TA instruments). The experiments were performed on 10 -15 mg samples over a temperature range of 0 – 175  $^\circ\text{C}$  at a constant heating rate of 10  $^\circ\text{C min}^{-1}$  with a purge of dry nitrogen flowing at 30  $\text{mL min}^{-1}$ . The samples were crushed, blotted dry and placed in crimped but vented aluminium pans for DSC experiments.

**Nitrogen Adsorption Isotherms.** Surface areas were measured by nitrogen adsorption and desorption at 77.3 K using a Autosorb IQ volumetric adsorption analyzer. Solid **3(I)** were degassed offline at room temperature  $^\circ\text{C}$  for 24 h under high vacuum  $10^{-6}$  mmHg, before analysis, followed by degassing on the analysis port under vacuum, for 30  $^\circ\text{C}$ . The isotherm of compound [**3**·AcOEt] was registered without previous treatment at vacuo.

**Single Crystal X-ray Diffraction.** Data were collected at 100K on a Bruker-Nonius FR591 Mo  $K\alpha$  rotating anode single crystal diffractometer equipped with an Apex II CCD area detector and Montel mirrors and an Oxford Cryostream Plus 700 Series. For the data collection the software *Apex2 V2010.7-0* (Bruker AXS 2010) was used. The data reduction was performed using Saint + Version 7.60A (Bruker AXS 2008) and the absorption correction using *SADABS V. 2008/1*<sup>1</sup> (CCDC 1012391, 101392, 101393, 101396, 101398 and 101399) and *TWINABS V. 2008/4*<sup>2</sup> (CCDC 1012389, 1063714, 101394, 101395 and 101397). The structures were solved using the program *SIR2011*<sup>3</sup> and refined by full matrix least squares using *SHELXL-97*<sup>4</sup> (CCDC 101389-101394 and 101399) and *SHELXL2013*<sup>4</sup> (CCDC 101395-101398).

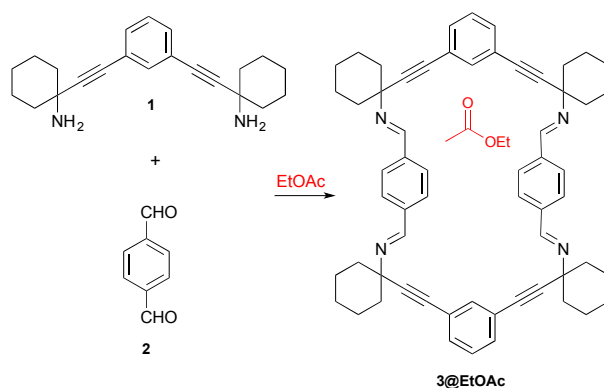
In order to gain greater insight into the disordered structure of the starting solvate, the X-ray structure of **3@EtOAc** was acquired at higher resolution (CCDC no. 1012389) Data collection: full sphere single crystal X-ray diffraction data were collected at 90 K on a Rigaku XtaLab P200 Mo  $K\alpha$  rotating anode equipped with a Pilatus 200K detector and an Oxford Cryostream 700 low temperature device. For data collection, data reduction and absorption correction the software CrystalClear 2.1 B29 (Rigaku, 2013)<sup>5</sup> was used. The structure was solved using the program *SIR2014*<sup>6</sup> and refined using *SHELXTL* Version 2014/3.<sup>7</sup>

## 1b. Materials and synthesis

### Materials

Ethyl acetate (EtOAc) HPLC quality purchased from Scharlau or Aldrich was used as received. 1,3-bispropargylic diamine **1** was prepared as described previously.<sup>8</sup> Terephthalaldehyde **2** and all other chemicals were purchased from Sigma-Aldrich and used as received.

### Synthesis of the macrocyclic tetraimine **3@EtOAc** solvated and the apohost **3(I)**



The macrocyclic tetraimine **3** was prepared by slow Schiff condensation of the diamine **1**<sup>8</sup> with terephthalaldehyde **2**. A typical procedure was as follows: a solution of the diamine **1** (400 mg, 1.248 mmol) and the dialdehyde **2** (169 mg, 1.248 mmol) in 120 mL of AcOEt was placed in a 250 mL erlenmeyer flask. The flask was covered with parafilm and let aside at room temperature for evolution. After four to ten weeks, prismatic crystals of **3@EtOAc** separated slowly from the solution. The crystals were harvested carefully from the bottom of the flask using a spatula, washed with fresh EtOAc and dried in the air to give an initial crop of **3@EtOAc** (135 mg, 15 % yield). Further quantities were obtained in successive crops from the mother solution to reach *c.a.* (410 mg, 50% yield).

Crystals of **3@EtOAc** (CCDC no. 1012389) are soluble in mesitylene and slightly soluble in chloroform but insoluble in a variety of common organic solvents such as: methanol, ethanol, dimethylsulfoxide, ethyl acetate, diethyl ether, tetrahydrofuran, toluene and hexane. Other solvents already tested such as cyclohexane and dichloromethane cause degradation of the crystal integrity.

To prepare the unsolvated material **3(I)** (CCDC no. 1012398) crystals of **3@EtOAc** were evacuated at  $5 \times 10^{-2}$  mmHg at room temperature for 12 h.

**3(I)**: <sup>1</sup>H NMR (CDCl<sub>3</sub>), m.p. > 250 °C (dec.).  $\delta$  (ppm from TMS): 8.82 (s, 4H), 7.88 (s, 8H), 7.68 (s, 2H), 7.47 (d,  $J = 7.5$  Hz, 4H), 7.32 (t,  $J = 7.8$  Hz, 2H), 1.82 (m, 20H). <sup>13</sup>C NMR in CDCl<sub>3</sub> ( $\delta$ , ppm): 157.7, 138.5, 134.6, 131.5, 128.7, 128.6, 123.7, 91.7, 88.8, 63.9, 39.8, 25.6, 23.2. ESI-HRMS (+)  $m/z$  (%): calc. C<sub>60</sub>H<sub>61</sub>N<sub>4</sub> 837.4896; exp. 837.4902 [M+H]. Anal. Calcd. for C<sub>60</sub>H<sub>60</sub>N<sub>4</sub>: C, 86.08; H, 7.22; N, 6.69. Found: C, 85.48; H, 7.17; N, 6.65.

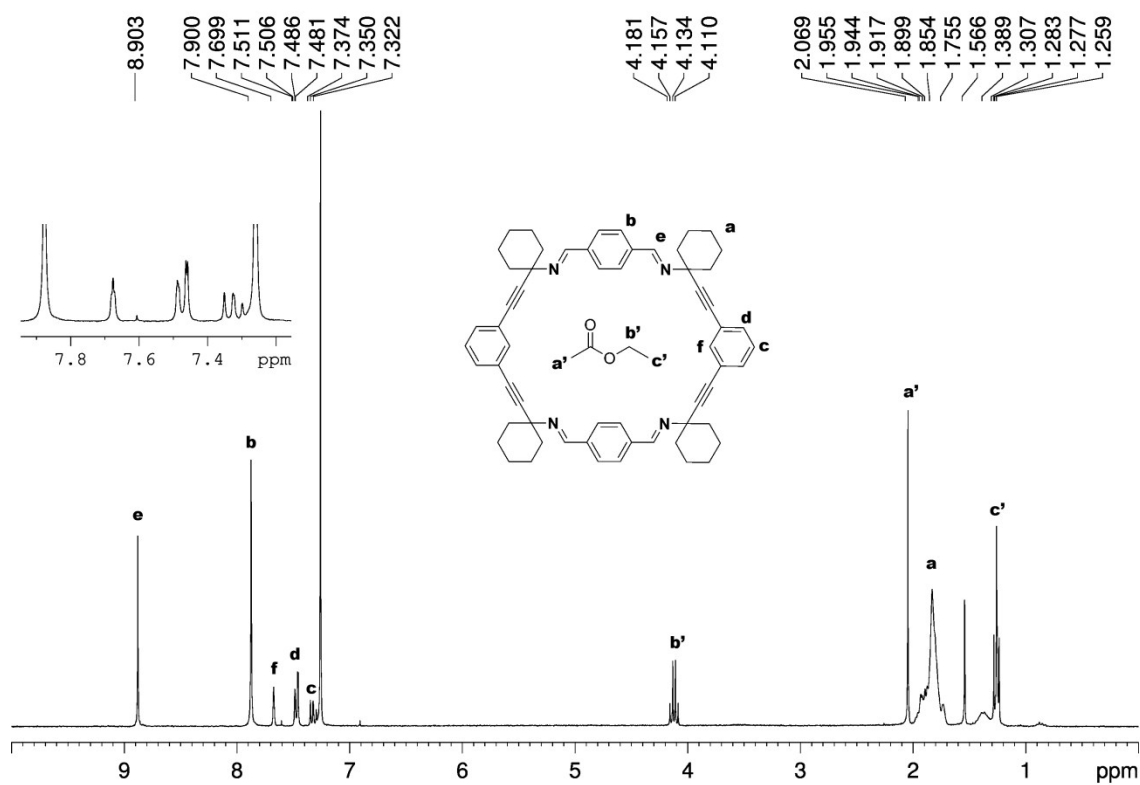


Figure S1 :  $^1\text{H}$  NMR spectrum of 3@EtOAc dissolved in  $\text{CDCl}_3$

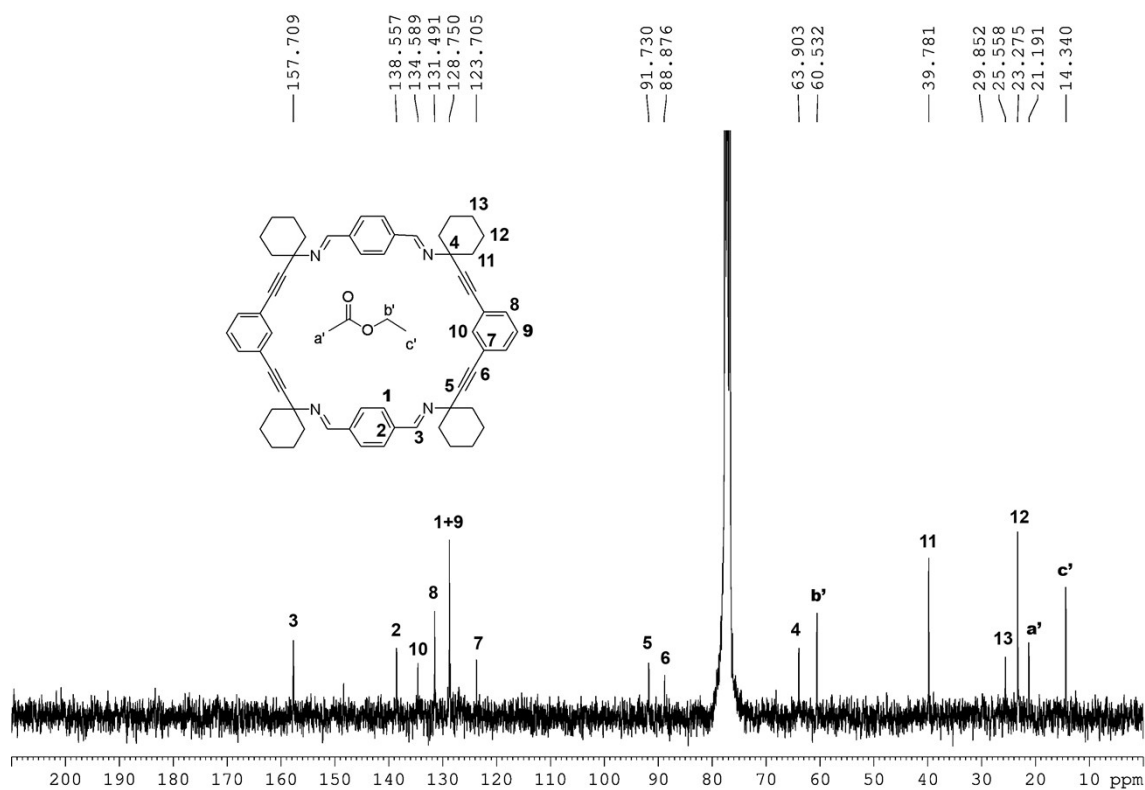


Figure S2 :  $^{13}\text{C}$  NMR spectrum of 3@EtOAc dissolved in  $\text{CDCl}_3$

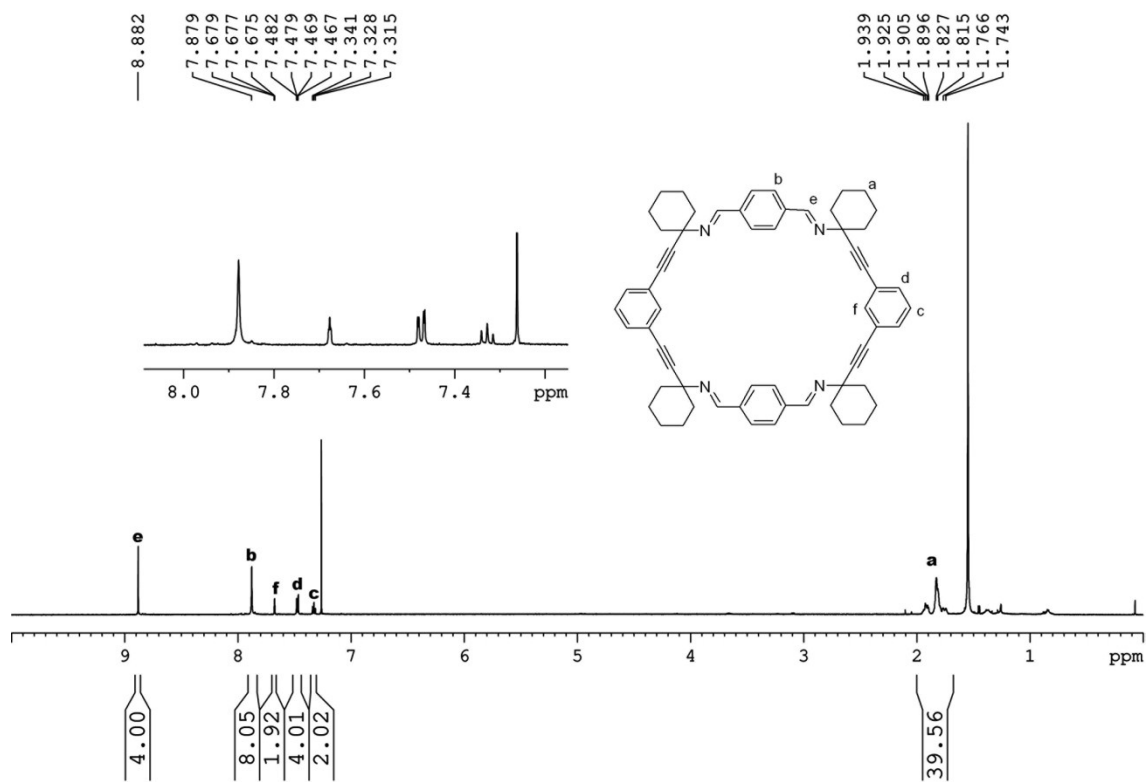


Figure S3 :  $^1\text{H NMR}$  spectrum of **3(I)** dissolved in  $\text{CDCl}_3$

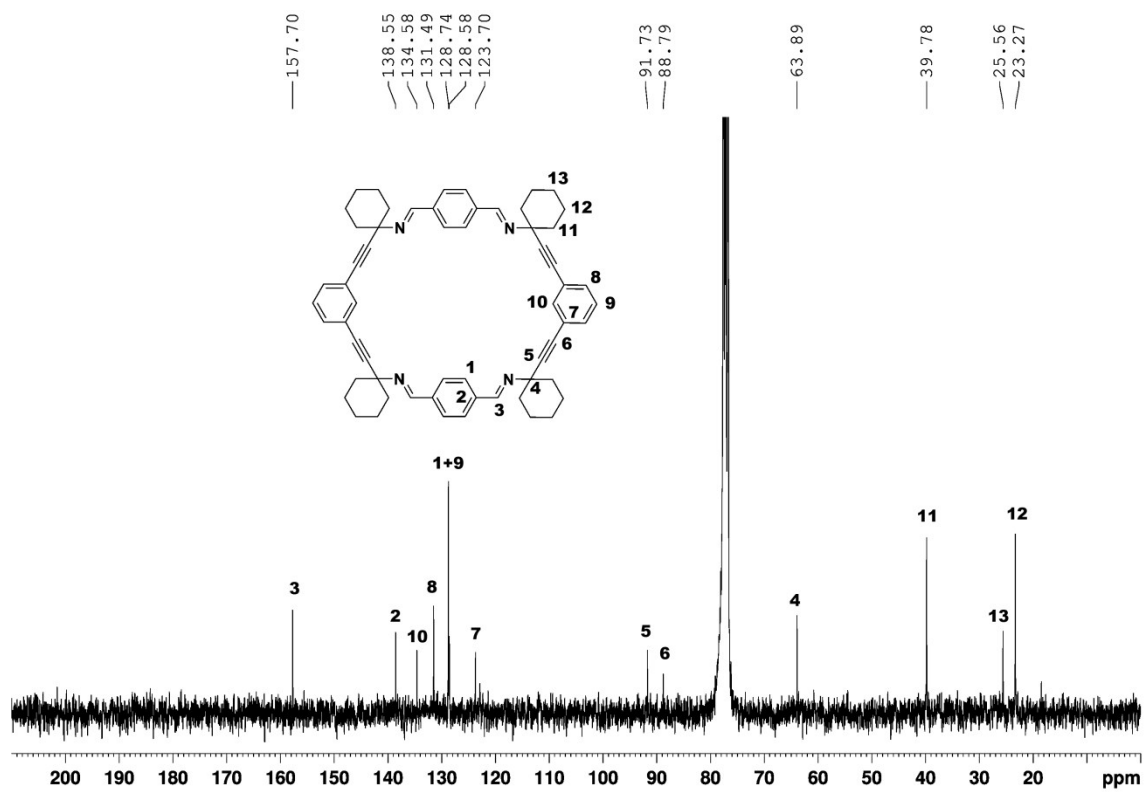
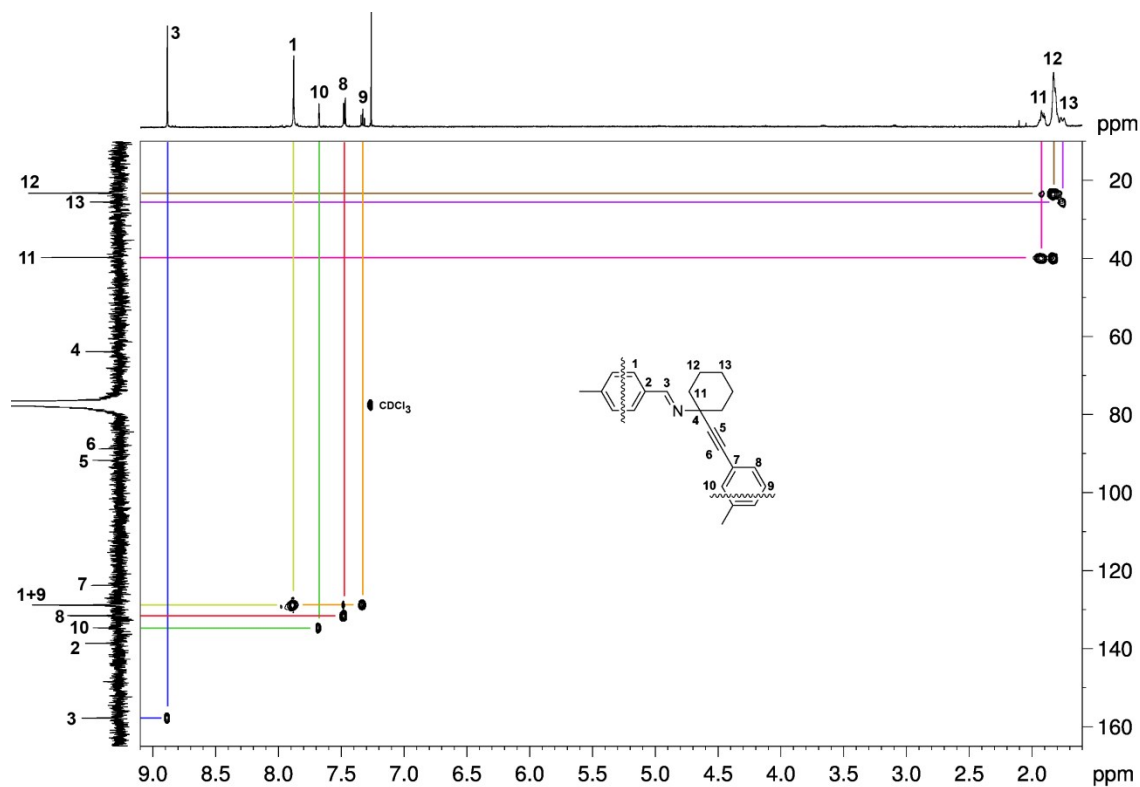
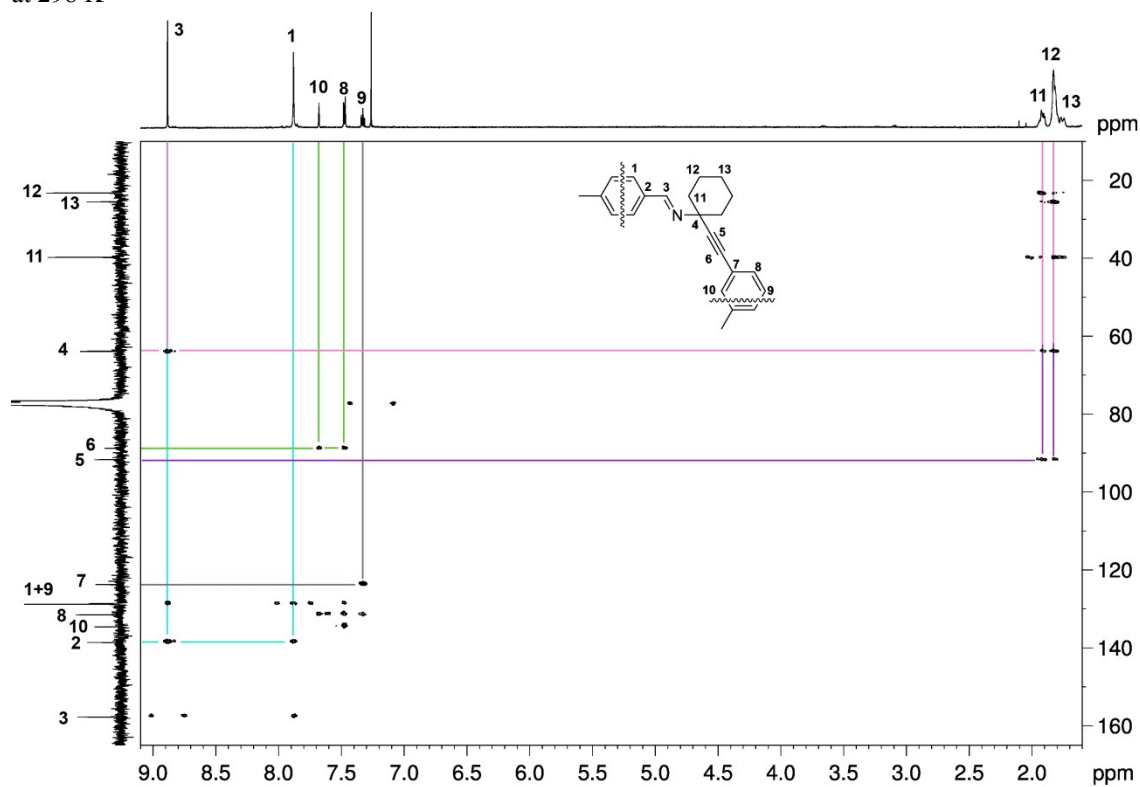


Figure S4 :  $^{13}\text{C NMR}$  spectrum of **3(I)** dissolved in  $\text{CDCl}_3$



**Figure S5:** Heteronuclear single quantum correlation (HSQC) spectrum of tetraimine **3(I)** in  $\text{CDCl}_3$  at 298 K



**Figure S6:** Heteronuclear multiple bond correlation (HMBC) spectrum of the tetraimine **3(I)** in  $\text{CDCl}_3$  at 298 K

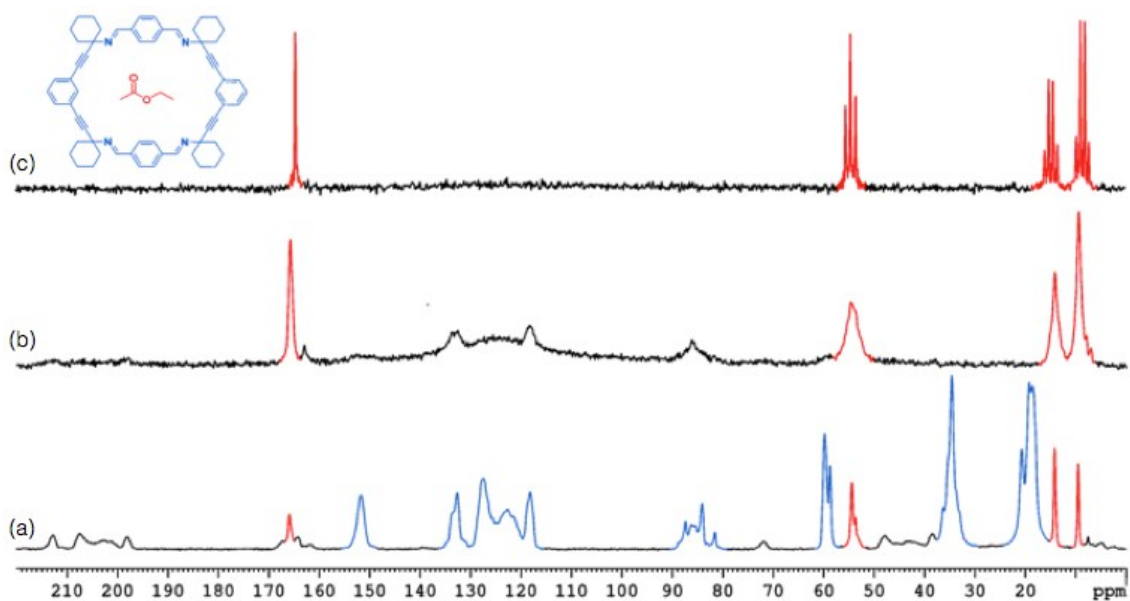


**Figure S7:** (a)  $^{13}\text{C}$  CP-MAS spectra of **3@EtOAc**, EtOAc peaks in red. (b)  $^1\text{H}$  undecoupled normal mode (without cross polarization)  $^{13}\text{C}$  MAS spectra **3@EtOAc**. In this mode, only the mobile EtOAc peaks appear (in red) (c)  $^1\text{H}$  undecoupled normal mode  $^{13}\text{C}$  MAS spectra of liquid AcOEt.

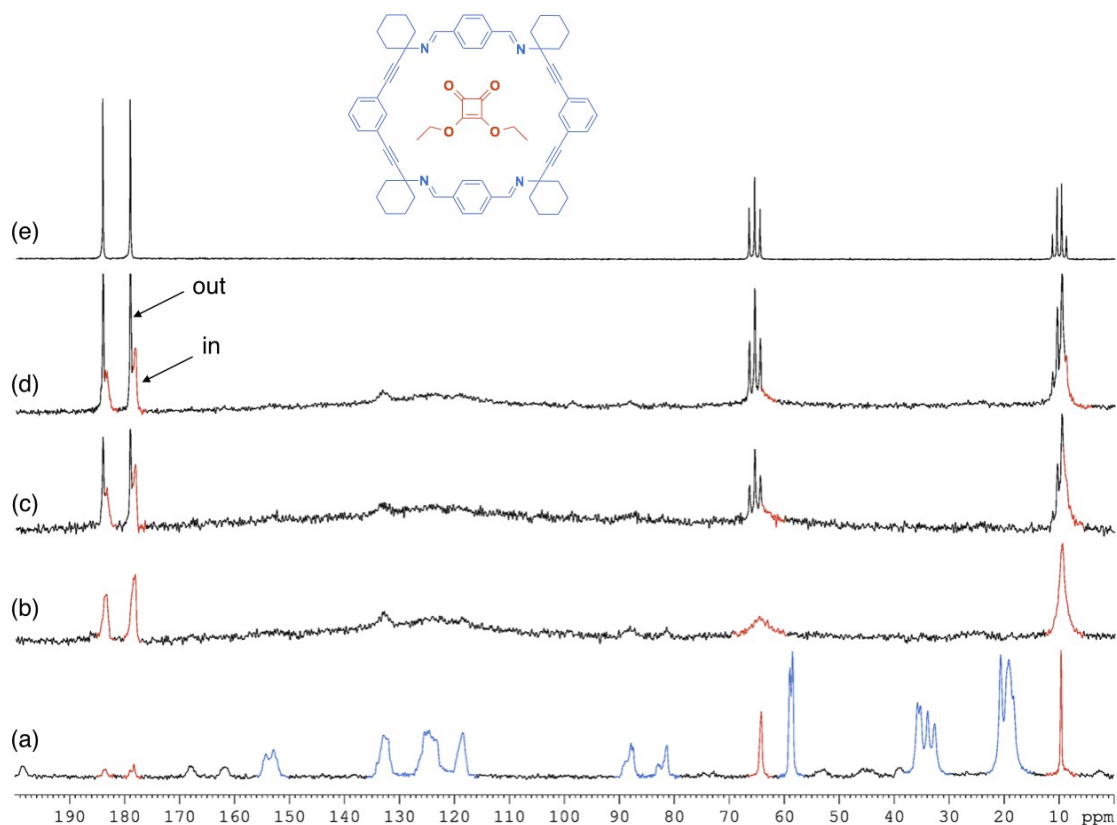


**Figure S8:** (a)  $^{13}\text{C}$  CP-MAS ( $^{13}\text{C}$ - $^1\text{H}$ , decoupled) spectrum of **3@Diethyl squarate** (50 mg), diethyl squarate peaks in red. (b)  $^1\text{H}$  undecoupled normal mode (without cross polarization)  $^{13}\text{C}$  MAS spectrum of **3@Diethyl squarate**. In this mode, only the included diethyl squarate resonances appeared as broad peaks (in red) (c) *Idem*, after addition of 2  $\mu\text{L}$  of liquid diethyl squarate; (d) *Idem*, after addition of 4  $\mu\text{L}$  of liquid diethyl squarate; (e)  $^1\text{H}$  undecoupled normal mode  $^{13}\text{C}$  MAS spectra of liquid diethyl squarate.



## TGA and DSC

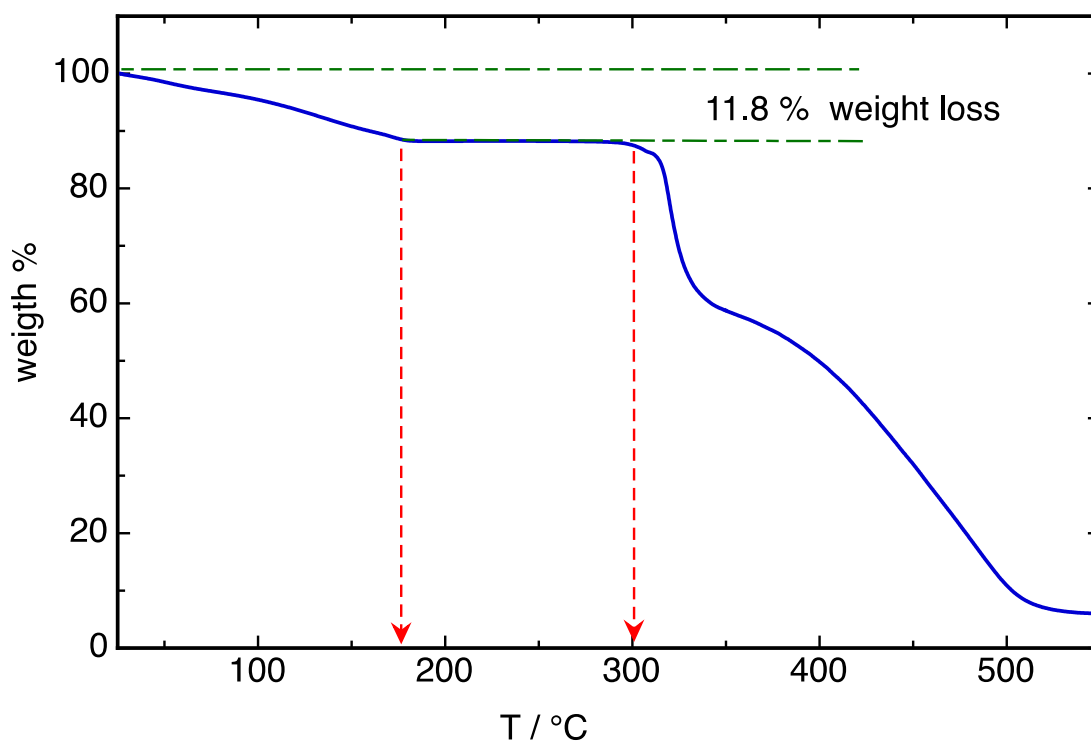


**Figure S9:** Thermogravimetric analysis of **3@EtOAc**. A  $10\text{ }^{\circ}\text{C}\cdot\text{min}^{-1}$  ramp was used.

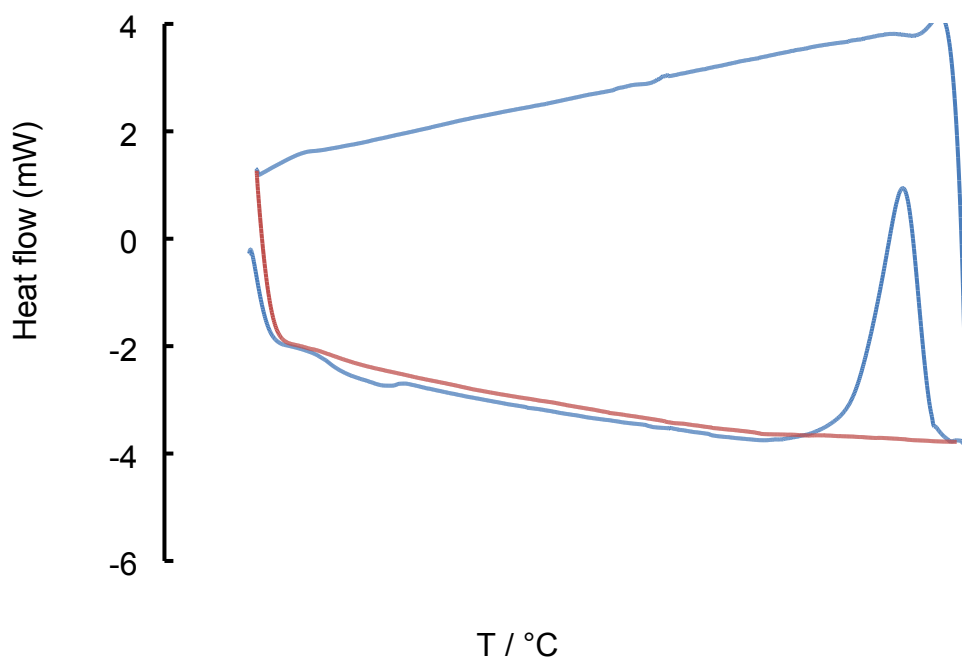


**Figure S10:** DSC trace of the empty crystal **3(I)** showing the irreversible transition occurring at  $177^{\circ}\text{C}$  (blue line). Second cycle (red). The analysis was run with a  $10\text{ }^{\circ}\text{C}\cdot\text{min}^{-1}$  ramp.

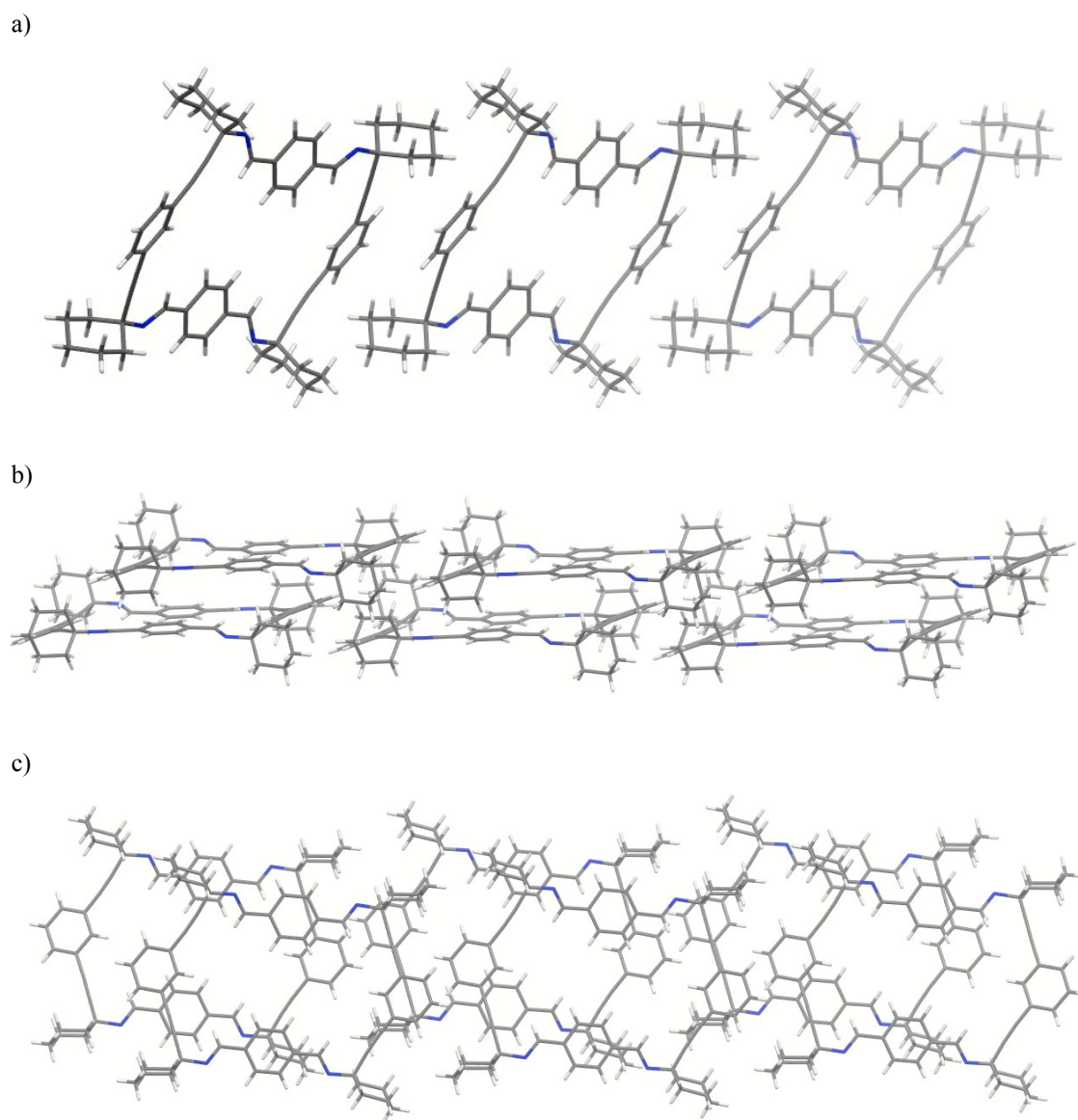


**Figure S11:** X-ray structure, (a) along the a-axis, (b) side view, (c) top view of the more dense, thermally stable, polymorph **3(II)** (triclinic, P-1,  $D_C = 1.127 \text{ g cm}^{-3}$ ; CCDC no. 1012399).

### Procedure for guest inclusion:

One single crystal of the vacuum treated crystallization harvest of the cycloimine was dipped in approx. 1mL of the neat solvent to be included in the channels of the solid. The period required for the diffusion of the guest into the solid is highly dependent on the guest sample. The exact range varies from less than five minutes for nitromethane to 48-72 h for nicotine and stilbene. After this period, the crystal was removed and rapidly cooled to – 100 K before the X-ray diffraction analysis.

### Crystal Data of solvates

Crystal data for **3@S(-)-Nicotine** (CCDC no.1063714):  $C_{70}H_{74}N_6$ ,  $M = 999.34$ , monoclinic,  $a = 35.689(4)$  Å,  $b = 5.9481(6)$  Å,  $c = 28.840(3)$  Å,  $\alpha = 90^\circ$ ,  $\beta = 97.562(6)^\circ$ ,  $\gamma = 90^\circ$ ,  $V = 6069.0(11)$  Å<sup>3</sup>,  $T = 100(2)$  K, space group  $C2$ ,  $Z = 4$ , 90524 reflections measured, 17187 independent reflections ( $R_{int} = 0.1126$ ). The final  $R_I$  values were 0.0768 ( $I > 2\sigma(I)$ ). The final  $wR(F^2)$  values were 0.2101 ( $I > 2\sigma(I)$ ). The final  $R_I$  values were 0.0931 (all data). The final  $wR(F^2)$  values were 0.2312 (all data).

Crystal data for **3@Nitromethane** (CCDC no.1012393):  $C_{63}H_{69}N_7O_6$ ,  $M = 1020.25$ , monoclinic,  $a = 34.875(4)$  Å,  $b = 5.7940(6)$  Å,  $c = 28.028(3)$  Å,  $\alpha = 90.00^\circ$ ,  $\beta = 98.453(2)^\circ$ ,  $\gamma = 90.00^\circ$ ,  $V = 5602.0(10)$  Å<sup>3</sup>,  $T = 100(2)$  K, space group  $C2/c$ ,  $Z = 4$ , 39875 reflections measured, 11756 independent reflections ( $R_{int} = 0.0370$ ). The final  $R_I$  values were 0.0610 ( $I > 2\sigma(I)$ ). The final  $wR(F^2)$  values were 0.1765 ( $I > 2\sigma(I)$ ). The final  $R_I$  values were 0.0742 (all data). The final  $wR(F^2)$  values were 0.1876 (all data).

Crystal data for **3@Diethyl squarate** (CCDC no.1012391):  $C_{68}H_{71}N_4O_{4.50}$ ,  $M = 1016.29$ , monoclinic,  $a = 34.814(2)$  Å,  $b = 5.8498(4)$  Å,  $c = 27.956(2)$  Å,  $\alpha = 90.00^\circ$ ,  $\beta = 98.517(2)^\circ$ ,  $\gamma = 90.00^\circ$ ,  $V = 5630.7(7)$  Å<sup>3</sup>,  $T = 100(2)$  K, space group  $C2/c$ ,  $Z = 4$ , 68338 reflections measured, 16500 independent reflections ( $R_{int} = 0.0255$ ). The final  $R_I$  values were 0.0579 ( $I > 2\sigma(I)$ ). The final  $wR(F^2)$  values were 0.1626 ( $I > 2\sigma(I)$ ). The final  $R_I$  values were 0.0733 (all data). The final  $wR(F^2)$  values were 0.1751 (all data).

Crystal data for **3@p-Xylene** (CCDC no.1012395):  $C_{68}H_{70}N_4$ ,  $M = 943.28$ , triclinic,  $a = 5.8032(7)$  Å,  $b = 17.6171(18)$  Å,  $c = 28.095(3)$  Å,  $\alpha = 82.852(4)^\circ$ ,  $\beta = 89.950(4)^\circ$ ,  $\gamma = 81.848(4)^\circ$ ,  $V = 2820.8(5)$  Å<sup>3</sup>,  $T = 100(2)$  K, space group **PError!**,  $Z = 2$ , 10911 reflections measured, 10911 independent reflections ( $R_{int} = 0.0751$ ). The final  $R_I$  values were 0.0788 ( $I > 2\sigma(I)$ ). The final  $wR(F^2)$  values were 0.1961 ( $I > 2\sigma(I)$ ). The final  $R_I$  values were 0.1480 (all data). The final  $wR(F^2)$  values were 0.2277 (all data).

Crystal data for **3@Ethylene glycol** (CCDC no.1012392):  $C_{63}H_{69}N_4O_3$ ,  $M = 930.22$ , monoclinic,  $a = 34.994(5)$  Å,  $b = 5.7712(9)$  Å,  $c = 28.005(5)$  Å,  $\alpha = 90.00^\circ$ ,  $\beta = 97.696(5)^\circ$ ,  $\gamma = 90.00^\circ$ ,  $V = 5604.9(15)$  Å<sup>3</sup>,  $T = 100(2)$  K, space group  $C2/c$ ,  $Z = 4$ , 20328 reflections measured, 9168 independent reflections ( $R_{int} = 0.0449$ ). The final  $R_I$  values were 0.0681 ( $I > 2\sigma(I)$ ). The final  $wR(F^2)$  values were 0.1908 ( $I > 2\sigma(I)$ ). The final  $R_I$  values were 0.0978 (all data). The final  $wR(F^2)$  values were 0.2163 (all data).

Crystal data for **3@p-Anisaldehyde** (CCDC no.1012394):  $C_{68}H_{68}N_4O_2$ ,  $M = 973.26$ , monoclinic,  $a = 35.119(8)$  Å,  $b = 5.8515(13)$  Å,  $c = 28.129(6)$  Å,  $\alpha = 90.00^\circ$ ,  $\beta = 96.944(5)^\circ$ ,  $\gamma = 90.00^\circ$ ,  $V = 5738(2)$  Å<sup>3</sup>,  $T = 100(2)$  K, space group  $C2/c$ ,  $Z = 4$ , 9090 reflections measured, 9090 independent reflections ( $R_{int} = 0.0999$ ). The final  $R_I$  values were 0.1199 ( $I > 2\sigma(I)$ ). The final  $wR(F^2)$  values were 0.3229 ( $I > 2\sigma(I)$ ). The final  $R_I$  values were 0.1489 (all data). The final  $wR(F^2)$  values were 0.3400 (all data).

Crystal data for **3@cis-Stilbene** (CCDC no.1012397):  $C_{74}H_{72}N_4$ ,  $M = 1017.35$ , triclinic,  $a = 5.8111(13)$  Å,  $b = 17.553(4)$  Å,  $c = 28.328(5)$  Å,  $\alpha = 82.080(6)^\circ$ ,  $\beta = 89.417(6)^\circ$ ,  $\gamma = 83.086(6)^\circ$ ,  $V = 2841.2(10)$  Å<sup>3</sup>,  $T = 100(2)$  K, space group **PError!**,  $Z = 2$ , 21469 reflections measured, 21469 independent reflections ( $R_{int} = 0.0621$ ). The final  $R_I$  values were 0.0949 ( $I > 2\sigma(I)$ ). The final  $wR(F^2)$  values were 0.2375 ( $I > 2\sigma(I)$ ). The final  $R_I$  values were 0.1388 (all data). The final  $wR(F^2)$  values were 0.2665 (all data).

Crystal data for **3@R-(+)-Limonene** (CCDC no.1012396):  $C_{70}H_{76}N_4$ ,  $M = 973.34$ , monoclinic,  $a = 34.833(4)$  Å,  $b = 5.8219(7)$  Å,  $c = 28.205(3)$  Å,  $\alpha = 90^\circ$ ,  $\beta = 98.490(5)^\circ$ ,  $\gamma = 90^\circ$ ,  $V = 5657.1(12)$  Å<sup>3</sup>,  $T = 100(2)$  K, space group  $C2$ ,  $Z = 4$ , 25503 reflections measured, 11682 independent reflections ( $R_{int} = 0.0803$ ). The final  $R_I$  values were 0.0699 ( $I > 2\sigma(I)$ ). The final  $wR(F^2)$  values were 0.1761 ( $I > 2\sigma(I)$ ). The final  $R_I$  values were 0.1361 (all data). The final  $wR(F^2)$  values were 0.2142 (all data).

Representative geometric parameters of solvates **3**@guest (L; W1; W2)

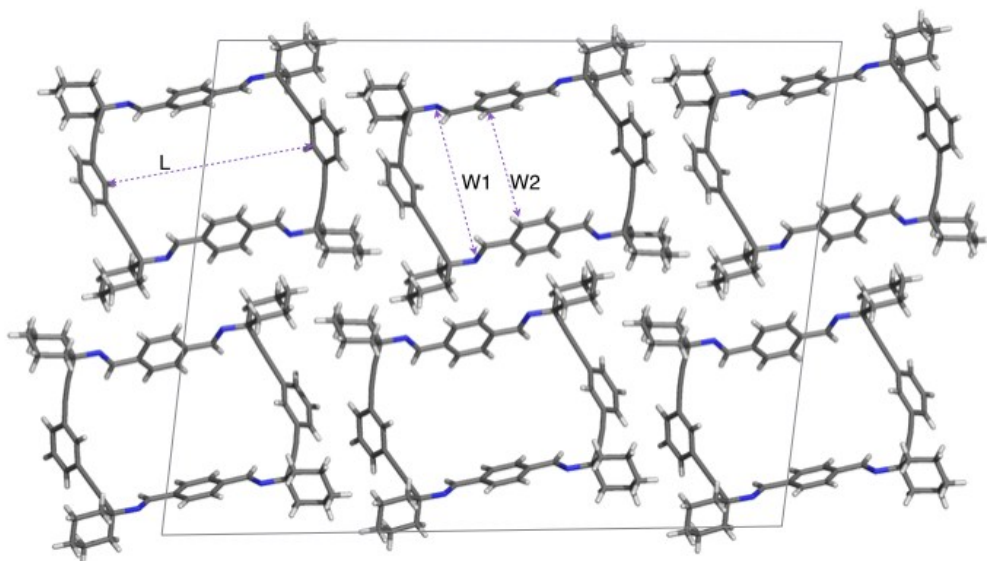


**Table S1.** Comparison of stoichiometry (S), calculated density ( $D_C$ ) and pore dimensions: length (L) and width (W1 and W2) of different inclusion complexes

	Structure	CCDC No	S <sup>a</sup>	$D_C$ <sup>b</sup> g cm <sup>-3</sup>	L Å	W1 Å	W2 Å
1	<b>3(I)</b> <sup>c</sup>	1012398	–	0.99	11.98	9.20	6.90
2	<b>3(II)</b> <sup>d</sup>	1012399	–	1.13	12.14	9.91	5.54
3	<b>3@EtOAc</b>	1012389	3:4	1.12	11.97	9.23	6.11 - 6.91 <sup>g</sup>
4	<b>3(I)@S(-)-Nicotine</b> <sup>f</sup>	1063714	1:1	1.09	12.22	9.52	7.35
5	<b>3@Diethyl Squarate</b>	1012391	1:1	1.20	11.97	9.11	6.66
6	<b>3@Ethylene Glycol</b>	1012392	2:3	1.11	12.06	9.09	6.12 - 6.71 <sup>g</sup>
7	<b>3@Nitromethane</b>	1012393	1:3	1.21	12.10	9.09	6.67
8	<b>3@p-Anisaldehyde</b>	1012394	1:1	1.20	12.00	9.34	6.35 - 7.34 <sup>g</sup>
9	<b>3@p-Xylene</b>	1012395	2:3	1.11	12.00	9.18	6.72
10	<b>3(I)@Z-Stilbene</b> <sup>e</sup>	1012397	1:1	1.01	12.02	9.34	7.57
11	<b>3(I)@(R)-(+)-Limonene</b> <sup>f</sup>	1012396	1:1	1.14	12.01	9.21	6.92

<sup>a</sup> S = Crystallographic stoichiometry (**3**:guest) . <sup>b</sup> Crystallographic densities. <sup>c</sup> **3(I)**: Porous empty crystal. <sup>d</sup> **3(II)**: Non porous empty crystal, triclinic space group *P*-1, obtained by heating **3(I)** below to 160°C. <sup>e</sup> Obtained from **3(I)**, triclinic space group *P*-1. <sup>f</sup> Obtained from **3(I)**, space group *C*2 due to the asymmetry of the guest. <sup>g</sup> Indicate disorder of phenyl rings between two limiting positions.

### Quantitative determination of the molar ratio [3:sample] by <sup>1</sup>H NMR spectroscopy

A single monocrystal of **3@EtOAc** was soaked in 100 μL of guest (neat) for 72 h at room temperature. After this period, the solution was removed and the crystal was washed with EtOAc (2 × 0.5 mL) and MeOH (3 × 0.5 mL), respectively, and dried under vacuum for 10 minutes.

If the crystal was small (length < 0.5 mm) it was dissolved in 0.6 mL of CDCl<sub>3</sub> followed by <sup>1</sup>H NMR measurement. The stoichiometry of the crystal was determined based on the integral ratios of the signal of the imine protons and the corresponding protons of the guest molecule (see Figure S13). This procedure is slow (>24 h) and due to the poor solubility of cycloimine **3** it is only suitable for relatively small crystals (length < 0.2-0.3 mm).

For bigger crystals (length > 0.4 mm) the complete dissolution of the crystal in CDCl<sub>3</sub> was unsuitable due to the low solubility of **3** in CDCl<sub>3</sub>. In these cases, it was necessary the destruction of the imine macrocycle **3** by adding 50 μL of DCl/D<sub>2</sub>O (37%) to the sample and , then diluting with a mixture of DMSO-*d*<sub>6</sub>:CDCl<sub>3</sub> (2.5:1 v/v, 600 μL). The stoichiometries of the inclusion complexes were determined based on the integral ratios of well-separated proton signals of the macrocyclic tetraimine and the guest (i.e. protons of the resulting dialdehyde from **3**) (see Figure S14).

**Table S2.** Comparison of molar ratios [3:guest] obtained by X-ray diffraction and <sup>1</sup>H NMR of the different inclusion complexes

Sample	Sample Volume <sup>a</sup> Å <sup>3</sup>	Solvate	Crystallographic molar ratio <sup>b</sup>	<sup>1</sup> H-NMR molar ratio <sup>c</sup>
EtOAc	100,7	<b>3@AcOEt</b>	1:1.34	1:1.36
S-(-)-Nicotine	187,0	<b>3(I)@S-(-)-Nicotine<sup>f</sup></b>	1:1	1:0.90
Diethyl Squarate	173,5	<b>3@Diethyl Squarate</b>	1:1	1:1.04
Ethylene glycol	66,7	<b>3@Ethylene Glycol</b>	1:1.5	1:1.54
Nitromethane	55,6	<b>3@Nitromethane</b>	1:3	1:3.4
<i>p</i> -Anisaldehyde	147,8	<b>3@p-Anisaldehyde</b>	1:1	1:0.93
<i>p</i> -Xylene	136,2	<b>3@p-Xylene</b>	1:1.5	1:1.24
Z-Stilbene	216,0	<b>3(I)@Z-Stilbene<sup>e</sup></b>	1:1	1:0.8
R-(+)-Limonene	177,3	<b>3(I)@(R)-(+)-Limonene<sup>f</sup></b>	1:1	1:0.96

<sup>a</sup> CPK molecular volumes were calculated from DFT (EDF1) energy-minimized structures using MacSpartan'14 (v. 1.1.4). <sup>b</sup> Calculated from the crystallographic formula. <sup>c</sup> Calculated by integration of the corresponding proton signals.

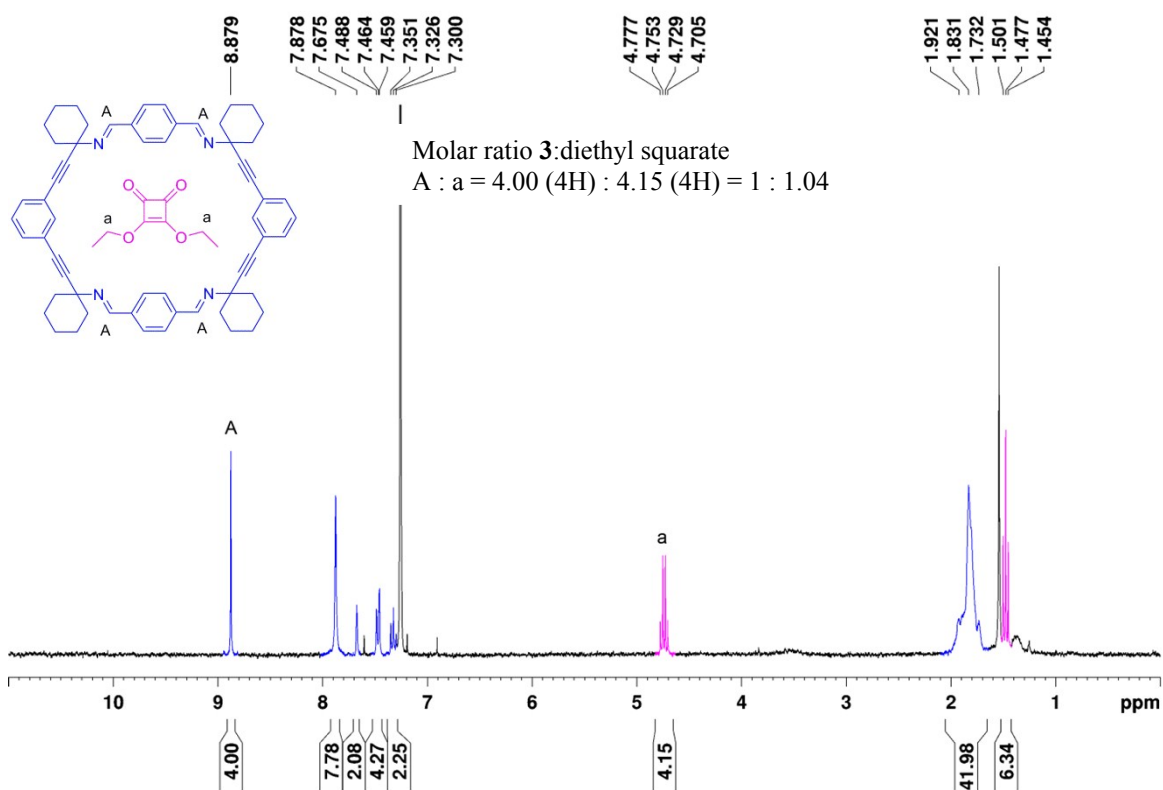


Figure S12: Molar ratio of 3:guest determined by direct dissolution of the inclusion complex in  $\text{CDCl}_3$ .

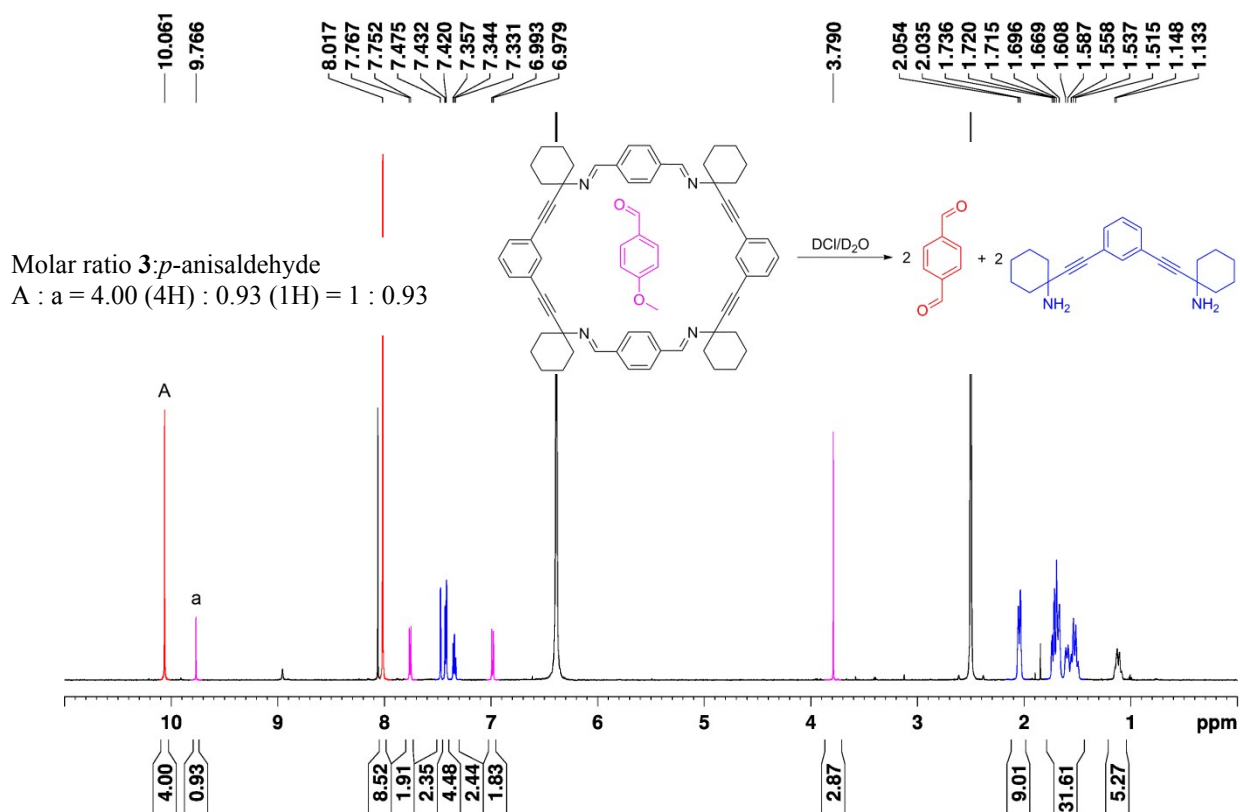


Figure S13: Molar ratio of 3:guest determined by previous hydrolysis of the cycloimine 3 in  $\text{DCI}/\text{D}_2\text{O}$ .

## 2. Theoretical Methods

### Theoretical methods.

The 1:1 complexes were completely optimized at the BP86-D3/def2-SVP and BP86-D3/def2-TZVP levels of theory using Turbomole 6.4 program.<sup>9</sup> The substitution, diffusion and cooperativity studies were performed only at the BP86-D3/def2-SVP level of theory due to the large number of atoms. In these studies, a model of the channel (formed by three host units) is used, which has been constructed from the crystallographic coordinates and kept frozen during the optimizations.

We have used the NCI method<sup>10</sup> to study the noncovalent interactions observed in the host-guest complexes. This method relies on two scalar fields to map local bonding properties: the electron density ( $\rho$ ) and the reduced-density gradient (RDG,  $\square$ ). It is able of mapping real-space regions where non-covalent interactions are important and is based exclusively on the electron density and its gradient. The information provided by NCI plots is essentially qualitative, i.e. which molecular regions interact. The color scheme is a red-green-blue scale with red for  $\rho^+$ cut (repulsive) and blue for  $\rho^-$ cut (attractive).

**Channel-Guest interactions.** The interaction energies of the channel and three different guests were computed from a macrocycle trimer (denoted as **3CM**) that has been kept frozen during the optimizations at the BP86-D3/def2-SVP level of theory.

**Table S2.** Interaction energies ( $E$ , kcal mol<sup>-1</sup>) for complexes between the channel model **3CM** and three different guests at different stoichiometric ratios.

	n = 1	n = 2	n = 3
<b>3CM</b> ···(EtOAc) <sub>n</sub>	-17.1	-37.8	-60.5
<b>3CM</b> ···(SQA) <sub>n</sub>	-30.8	-65.1	-96.7

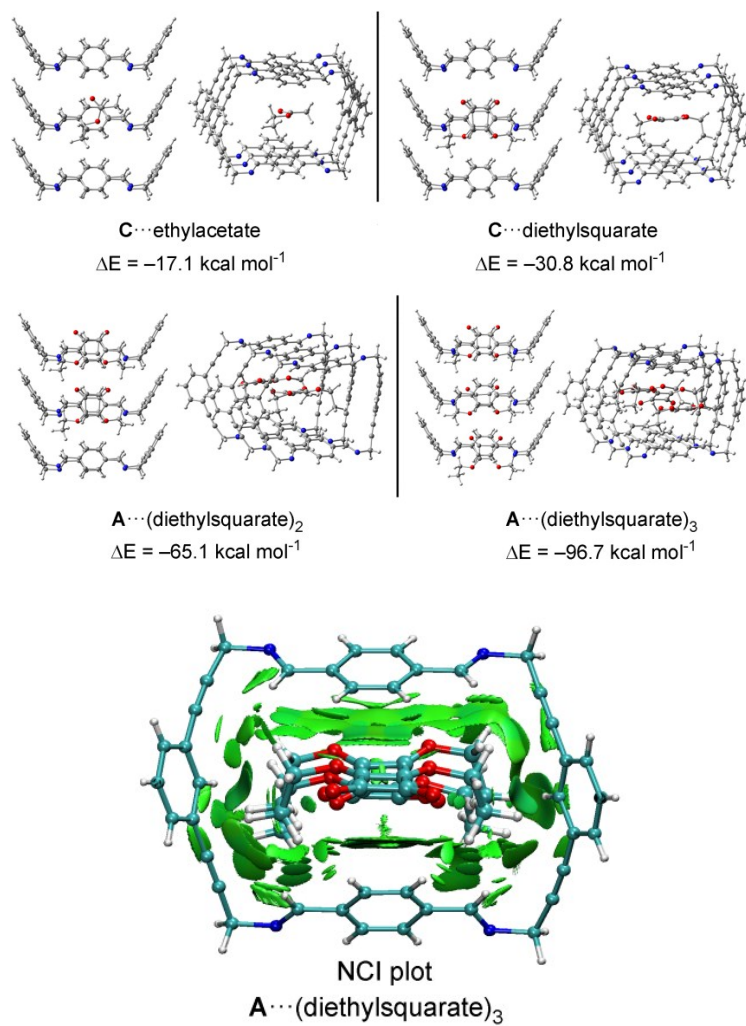


**Figure S14.** Optimized geometries of the complexes between the channel (**3CM**) and different guests. The NCI surfaces for the **3CM**...(SQA)<sub>n</sub> complex is also represented.



**Diffusion analysis.** To measure the facility of the guest to move inside the channel we have performed a DFT theoretical study (BP86-D3/def2-SVP) where we move the guest inside the channel as a reaction coordinate using steps separated by 1 Å and computing the interaction energy every step. In each point the energy of the system is relaxed (apart from the reaction coordinate) keeping the channel frozen. The diffusion energy estimated using this theoretical model is probably overestimated because the channel is not allowed to relax. However, our purpose is not to compute the exact diffusion barrier, instead we use the estimated energies for comparison purposes and provide qualitative results.

**Figures S15-S16** show the reaction coordinates for EtOAc and Diethyl Squarate moving inside the channel. The first point of the coordinate corresponds to the energy of the system locating the guest at more than 5 angstroms from the entrance of the channel. In the second point of the coordinate the guest is located at 2 Å away from the entrance and the reaction coordinate follows with steps of 1 Å and finishes when the guest is out of the channel at 4 Å from the exit.

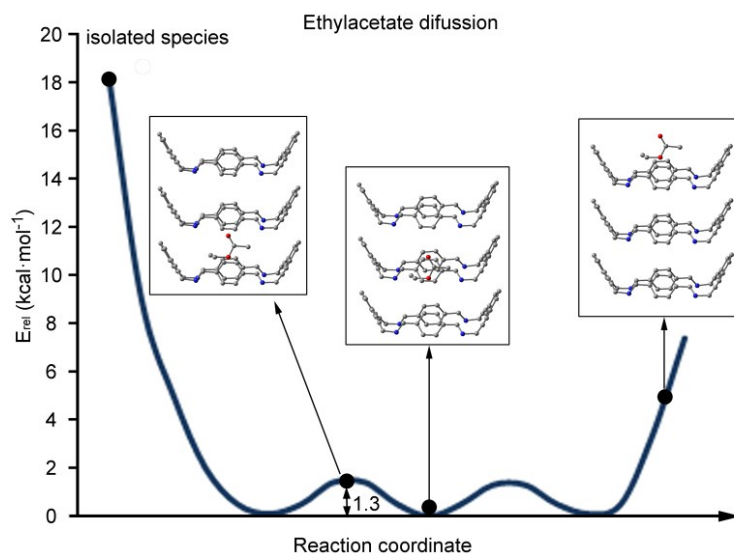


**Figure S15.** Reaction coordinate for EtOAc moving inside the channel. Hydrogen atoms have been omitted in the representation of several points of the coordinate. The diffusion barrier of ethylacetate is very small (1.3 kcal mol<sup>-1</sup>). Therefore it can freely move inside the channel with a high diffusion rate and is expected to be replaced by any of the other two guests easily and rapidly.

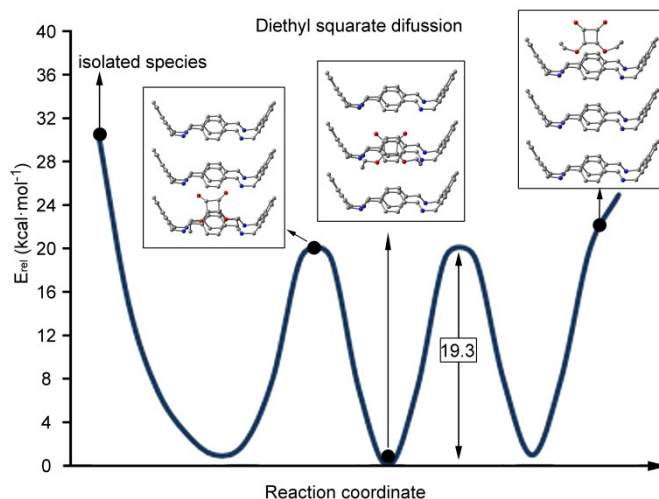


**Figure S16.** Reaction coordinate for diethylsquarate moving inside the channel. Hydrogen atoms have been omitted in the representation of several points of the coordinate. Diethylsquarate presents the highest diffusion barrier and the interaction energy is smaller than that of diethylphthalate.

#### Substitution analysis.

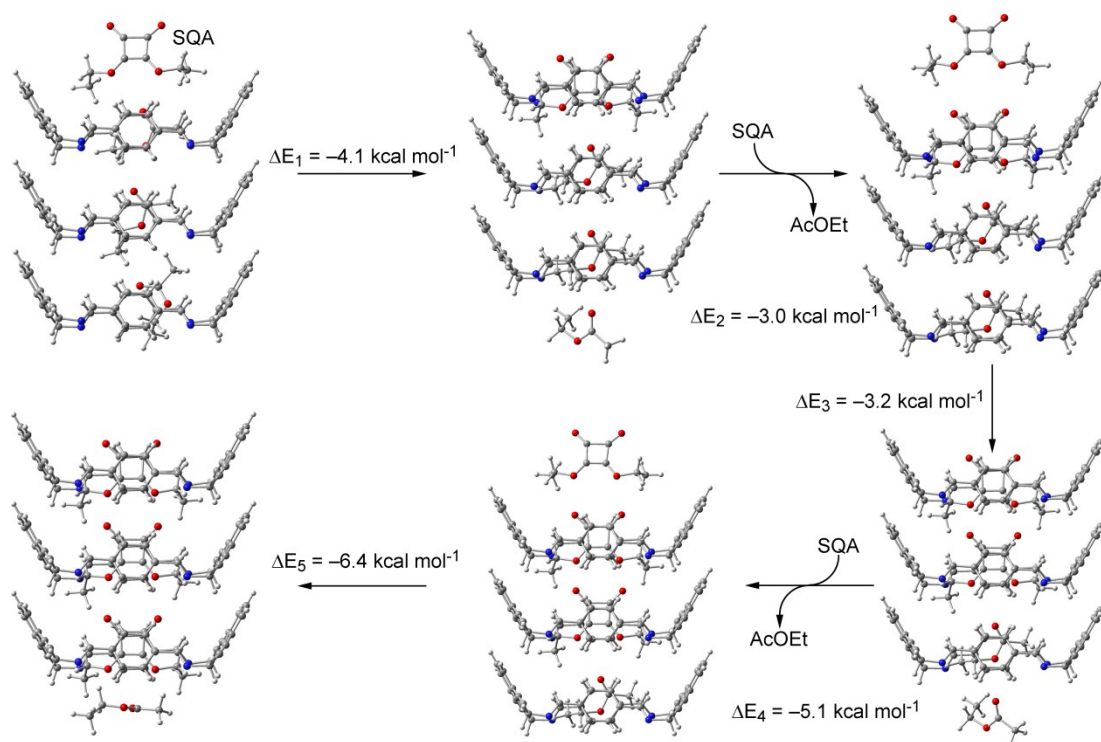


**Figure S17.** Proposed pathway for the progressive substitution of EtOAc by SQA and the energies associated to each step.

## References

- 1 G. M. Sheldrick, 2008.
- 2 M. C. Burla, R. Caliendo, M. Camalli, B. Carrozzini, G. L. Cascarano, C. Giacovazzo, M. Mallamo, A. Mazzone, G. Polidori, R. Spagna, *J. Appl. Cryst.* **2012**, *45*, 357-361.
- 3 G. M. Sheldrick, *Acta Cryst. A* **2008**, *64*, 112-122.
- 4 G. M. Sheldrick, SHELXL2013. University of Göttingen, Germany. **2013**.
- 5 J. W. Pflugrath, *Acta Crystallographica Section D-Biological Crystallography* **1999**, *55*, 1718-1725.
- 6 M. C. Burla, R. Caliendo, B. Carrozzini, G. L. Cascarano, C. Cuocci, C. Giacovazzo, M. Mallamo, A. Mazzone, G. Polidori, *J. Appl. Cryst.* **2015**, *48*, 306-309.
- 7 G. M. Sheldrick, *Acta Crystallographica Section C-Structural Chemistry* **2015**, *71*, 3-8.
- 8 B. Soberats, L. Martínez, M. Vega, C. Rotger, A. Costa, *Adv. Syn. Catal.* 2009, 351, 1727-1731.
- 9 R. Ahlrichs, M. Bär, M. Hacer, H. Horn, C. Kömel, *Chem. Phys. Lett.* 1989, 162, 165-169. (TURBOMOLE)
- 10 E. Johnson, S. Keinan, P. Mori-Sánchez, J. Contreras-García, A. Cohen, W. Yang, *J. Am. Chem. Soc.* 2010, 132, 6498-6506 (NCI).